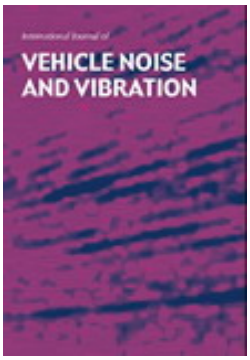

International Journal of Vehicle Noise and Vibration

ISSN online: 1479-148X - ISSN print: 1479-1471
https://www.inderscience.com/ijvnv

Simulation and experimental investigation of hydro-pneumatic energy harvesting suspension system

Magdy Naeem Awad, M.E. El-Arabi, Saber A. Rabbo, Mohamed I.B. Sokar

DOI: 10.1504/IJVNV.2023.10055211

Article History:
Received: 30 August 2022
Accepted: 02 November 2022
Published online: 10 April 2023

Simulation and experimental investigation of hydro-pneumatic energy harvesting suspension system

Magdy Naeem Awad*

Department of Mechanical Engineering Mechatronics Engineering,
Arab Academy for Science,
Technology and Maritime Transport,
Smart Village Campus, Giza, Egypt
Email: magdinaeem@hotmail.com
and
Mechatronics Engineering Department,
Canadian International College,
5th Settlement, Cairo, Egypt
*Corresponding author

M.E. El-Arabi

Department of Design and Production Engineering,
Faculty of Engineering,
Cairo University,
Cairo, Egypt
Email: prof_m_elaraby@yahoo.com

Saber A. Rabbo

Department of Mechanical Engineering,
Faculty of Engineering at Shoubra,
Benha University, Egypt
Email: saberabdrabbo@yahoo.com

Mohamed I.B. Sokar

Department of Mechanical Engineering,
Mechatronics Engineering,
Faculty of Engineering at Shoubra,
Benha University, Egypt
mail: mohamed.sokar@feng.bu.edu.eg

Abstract: This article describes a promising hydro-pneumatic regenerative suspension system (HPEHS) that converts the linear oscillation of the suspension system into rotational motion via a hydraulic rectifier to maintain a unidirectional rotational motion of a hydraulic motor connected to an electric generator to generate electricity. The simulation model using the block diagram-oriented environment of MATLAB-Simulink has been created based

on the governing equations to investigate the behaviour of the system and validate it. The effect of the sprung mass and the accumulator on the system performance and harvested power of the HPEHS system was investigated. It is found that the motor speed and harvested power increase with increasing sprung mass while the displacement of the sprung mass reduces. The existence of the accumulator in the system minimises the fluctuation in system pressure causing more stability to the suspension system. The average power of the regenerative suspension system is approximately 7.5 W.

Keywords: energy harvesting; hydro-pneumatic regenerative suspension; hydraulic rectifier.

Reference to this paper should be made as follows: Awad, M.N., El-Arabi, M.E., Rabbo, S.A. and Sokar, M.I.B. (2023) 'Simulation and experimental investigation of hydro-pneumatic energy harvesting suspension system', *Int. J. Vehicle Noise and Vibration*, Vol. 19, Nos. 1/2, pp.32–54.

Biographical notes: Magdy Naeem Awad received his PhD in Mechatronics Engineering from the Department of Mechanical Design and Production, Faculty of Engineering, Cairo University in 2020. He is currently working as an Assistant Professor in the Mechatronics Engineering Department of the Arab Academy for Science, Technology and Maritime Transport, Smart Village Campus, Giza, Egypt. His research concerns control engineering, system dynamics, and robotics.

M.E. El-Arabi received his PhD degree in 1969 in System Dynamics from the TIT University (Japan). He is a Professor of Design and Production Engineering at Cairo University (Egypt). His research interests include control engineering, system dynamic and fluid power systems

Saber A. Rabbo received his PhD degree in 1994 in Design and Production Engineering from Zagazig University. He is a Professor of Design and Production Engineering at Benha University (Egypt). His research interests include control engineering and robotics for a Mechatronics engineering.

Mohamed I.B. Sokar received his PhD degree in 2011 in Mechanical Engineering (Doktor der Ingenieurwissenschaften) from Faculty of Engineering, Institute of Fluid power drives and Control (IFAS), Aachen University, Germany. His research interests include analysis, simulation and design of efficient fluid power systems, and mechatronics.

1 Introduction

The suspension system of vehicles is exposed while travelling on uneven and curved roads to various disturbances, which requires a well-designed suspension system to give ride comfort. Conventional suspension systems are the link between wheels and car bodies, the parallel connection between hydraulic shock absorbers and springs allows them to absorb and dissipate vibrations into heat energy causing a large amount of energy to be wasted, while it can be recovered. A major factor in the modern vehicles industry is to harvest this wasted energy and converting into electricity.

The regenerative suspension systems can be classified based on how the vertical oscillations are converted into useful power. Energy recovery has been gaining

importance in recent years in systems subjected to an undesirable vibration. Among the designs that have received much attention are electromagnetic shock absorbers due to their high energy recovery capacity (Cassidy et al., 2011, Zuo and Zhang, 2013; Huang et al., 2015). The electromagnetic shock absorber structures are divided into two main categories, linear electromagnetic absorbers (Zhu et al., 2012; Zhang et al., 2018, 2012; Soares Dos Santos et al., 2016; Gysen et al., 2011; Zuo et al., 2010), and rotary electromagnetic absorbers (Liu et al., 2011; Tonoli et al., 2013; Hao and Namuduri, 2013). The rotating electromagnetic absorber designs rely on mechanical mechanisms to convert vertical motion into rotational motion to drive the electric generator. While linear electromagnetic absorbers use the linear motion caused by road vibrations to generate energy directly. The rotary electromagnetic absorbers based on mechanical transmission mechanisms can be smaller than linear absorbers and also have higher efficiency (Li and Zuo, 2013). Mechanical electromagnetic harvesters have been presented in many previous studies with different designs such as a mechanical ball screw actuator for converting linear vibration into rotational motion (Liu et al., 2017; Sabzehgar et al., 2014; Kim et al., 2016), rack and pinion gear set mechanism (Chen et al., 2018, Guo et al., 2016; Li et al., 2013a, 2013b), and other transmission gears mechanisms based on a mechanical motion rectifier (Maravandi and Moallem, 2015; Berg et al., 2014; Zhang et al., 2016). The hydraulic regenerative shock absorbers have also received a lot of attention recently because of their efficiency and ability to harvest energy from road vibrations. Mainly, the hydraulic regenerative shock absorbers can be classified as single-acting regenerative shock absorbers (Zhou et al., 2015; Xu et al., 2015; Awad and Me El-Arabi, 2021) and double-acting regenerative shock absorbers (Zhang et al., 2015; Li et al., 2014). The hydraulic regenerative shock absorbers mainly consist of three components. They are the hydraulic rectifier that ensures a one-way flow during shock absorber motion, the hydraulic motor that converts the hydraulic power to mechanical power, and the rotary electromagnetic generator that is responsible to harvest the electrical power (Awad et al., 2018a; Galluzzi et al., 2018). The double-acting regenerative shock absorber can give greater damping force during the compression and extension stages, the active working areas are the piston area and the annulus area of the rod side, respectively. On the contrary, the single-acting shock absorber relies on only one chamber (Awad et al., 2018b). Although several studies have discussed theoretically or by simulation different designs of suspension systems with or without energy regeneration. However, most of the previous studies do not take into account the two-way hydro-pneumatic energy harvesting design for the suspension system. Several practical questions still arise. To answer all these questions, an experimental study and a simulation model of the regenerative suspension system were conducted.

The contributions of this work can be namely summarised as follows:

- A unique experimental design for a hydro-pneumatic energy harvesting suspension system is suggested. This design is based on converting the linear vibrational motion of the suspension system into hydraulic power and finally to useful electric power.
- A MATLAB-Simulink model is performed and a comparison of the important variables that describe the system performance is obtained to validate the proposed experimental setup.

- The performance of the proposed HPEHS for various sprung masses is carried out to study the effect of change of sprung mass on the amount of energy that can be harvested.
- The operation of the hydro-pneumatic energy harvesting suspension system with and without an accumulator is performed to identify the importance of the accumulator in the hydraulic circuit of the HPEHS.

2 System description and mathematical model

The system description of the hydro-pneumatic energy harvesting suspension system (HPEHS) is analysed in this section. Then, the mathematical model of the individual system components is introduced to analyse the suspension system performance. The schematic diagram of the quarter-vehicle integrated with the HPEHS is shown in Figure 1. The suspension system consists of a hydraulic double-acting cylinder loaded with a variable suspension load. The hydraulic rectifier is used to convert the bidirectional linear motion of the shock absorber into the one-way rotary motion of the hydraulic motor to maintain the maximum harvested power. Two bladder accumulators are connected to the input and output ports of the hydraulic motor to compensate for the oil shortage caused by the difference in the hydraulic cylinder chambers volume and reduce the flow pulsations through the hydraulic circuit. The high-pressure line of the hydraulic circuit is connected to the hydraulic motor to drive the electromagnetic generator via a coupling. The external load bank is connected to the electromagnetic generator to obtain the harvested power.

The development of the nonlinear model of the proposed system requires mathematical relationships between the pressure, flow rate, and volume for the hydraulic cylinder chambers and the accumulators as well as the oil flow rate through the hydraulic rectifier circuit, the hydraulic motor pressure, and the harvested power from the generator.

Figure 1 Schematic diagram of HPEHS (see online version for colours)

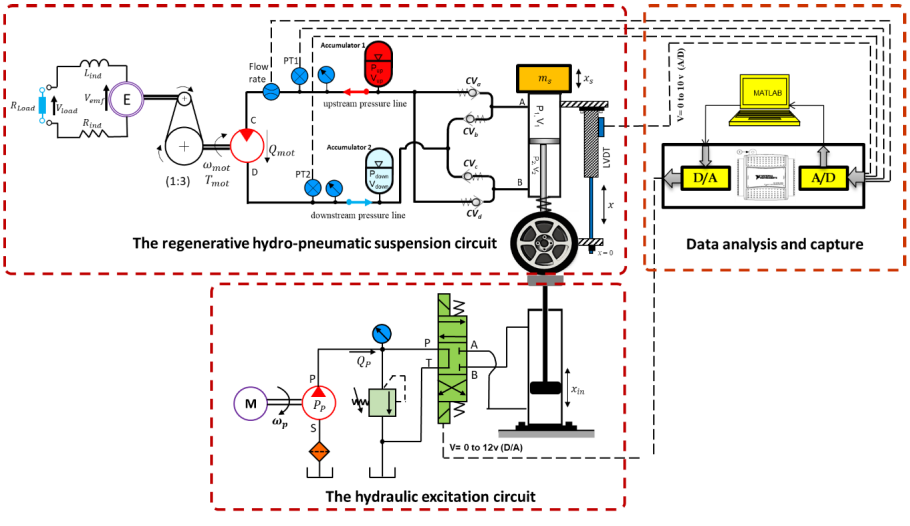

The present model is studied considering certain assumptions and conditions. The static suspension stage calculations are performed at a constant temperature of 20°C. Short transmission lines are used between the system components. Therefore, friction losses due to pipe length, oil compressibility, and inertia are neglected. The sprung mass directly acts over the suspension cylinder. The reference position of the suspension is considered at the middle of the cylinder stroke. There is no heat exchange between the accumulator gas and oil during the excitation stage.

2.1 Accumulator spring rate and piston forces analysis

The pressure and volume of the accumulators changed according to the subjected load on the suspension system. Under the static suspension force F_{st}, the pressure and volume of the accumulators will be changed isothermally to new pressure and new volume. When the suspension system is subjected to the road vibration force F_{road}, the pressure and volume of the accumulators will change in an adiabatic process. There are three states of the bladder accumulators as shown in Figure 2.

Figure 2 The three states of the upstream bladder accumulator (see online version for colours)

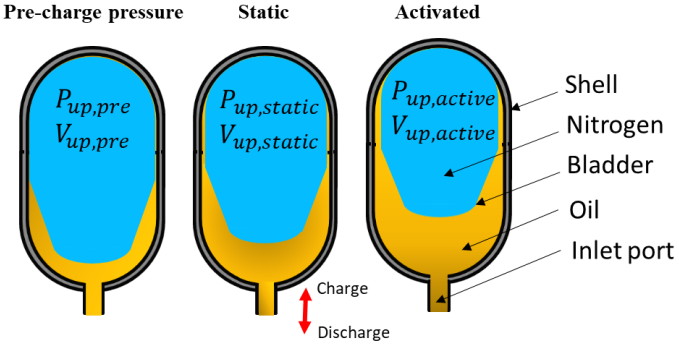

During the excitation stage, the relationship between the piston forces and chamber pressures can be expressed as:

$$F_1 = P_1 A_1 = P_{up,act} A_1 \tag{1}$$

$$F_2 = P_2 A_2 = P_{dn,act} A_2 \tag{2}$$

where P_1 is the pressure inside chamber 1, and P_2 is the pressure inside chamber 2, A_1 is the piston area, and A_2 is the annulus area of the rod side, the pressures inside accumulators 1 and 2 under the road vibration force are $P_{up,act}$ and $P_{dn,act}$ respectively.

While the suspension system is exposed to a static suspension load, the process is considered an isothermal process. The relationship between nitrogen pressure and nitrogen volume of the bladder can be expressed by the ideal gas equation:

$$P_{up,st} V_{up,st} = P_{up,pre} V_{up,pre} \tag{3}$$

$$P_{dn,st} V_{dn,st} = P_{dn,pre} V_{dn,pre} \tag{4}$$

where $P_{ur,st}$ and $P_{dn,st}$ are the pressure inside accumulators 1 and 2, $V_{up,st}$ and $V_{down,st}$ are the volume of accumulators 1 and 2 under the static suspension force, respectively, $P_{up,pre}$

and $P_{dn,pre}$ are the pre-charge pressure of accumulators one and two, $V_{up,pre}$ and $V_{dn,pre}$ are the initial volume of accumulators one and two, respectively. Based on the balance of piston forces under static suspension load:

$$F_{st} = P_{up,st} A_1 = P_{dn,st} A_2 \tag{5}$$

Under road excitation displacement x, the gas will be compressed to new volumes, which yields the following equations:

$$V_{up,act} = V_{up,st} - A_1 x \tag{6}$$

$$V_{dn,act} = V_{dn,st} + A_2 x \tag{7}$$

where $V_{up,act}$ and $V_{dn,ac}$ are the volume of accumulators one and two under the road vibration force, respectively. Utilising the state condition for an adiabatic process during the excitation stage:

$$P_{up,ac} V_{up,ac}^n = P_{up,st} V_{up,st}^n \tag{8}$$

$$P_{dn,ac} V_{dn,ac}^n = P_{dn,st} V_{dn,st}^n \tag{9}$$

where n is the specific heat ratio. The pressure force acting on the piston side can be obtained by solving equations (1), (3), (5), and (8):

$$F_1(x) = F_{st} \frac{\left(\dfrac{P_{dn,pre} V_{up,pre}}{F_{st}} \right)^n}{\left(\dfrac{P_{dn,pre} V_{up,pre}}{F_{st}} x \right)^n} \tag{10}$$

The pressure force acting on the rod side can be obtained by solving equations (2), (4), (5), and (9):

$$F_2(x) = F_{st} \frac{\left(\dfrac{P_{dn,pre} V_{dn,pre}}{F_{st}} \right)^n}{\left(\dfrac{P_{dn,pre} V_{dn,pre}}{F_{st}} + x \right)^n} \tag{11}$$

The spring rate for the hydro-pneumatic suspension cylinder can be described by the following equations.

The spring rate for the piston side:

$$k_1 = \frac{dF_1}{dx} = A_1 \frac{dP_1}{dx} \tag{12}$$

where

$$\frac{dp_1}{dx} = A_1 n P_{up,st} V_{up,st}^n \left(V_{up,st} - A_1 x \right)^{-n-1} \tag{13}$$

Substituting equations (3) and (5) into (12) yields:

$$k_1(x) = nF_{st} \frac{\left(\frac{P_{up,pre}V_{up,pre}}{F_{st}}\right)^n}{\left(\frac{P_{up,pre}V_{up,pre}}{F_{st}} - x\right)^{n+1}} \tag{14}$$

The spring rate for the rod side

$$k2 = \frac{dF_2}{dx} = A_2 \frac{dP_2}{dx} \tag{15}$$

$$\frac{dP_2}{dx} = -A_2 nP_{dn,st} \mid V_{dn,st}^n \left(V_{dn,st} + A_2 x\right)^{-n-1} \tag{16}$$

Combining equations (4), (5), and (15) results in

$$k_2(x) = -nF_{st} \frac{\left(\frac{P_{dn,pre}V_{dn,pre}}{F_{st}}\right)^n}{\left(\frac{P_{dn,pre}V_{dn,pre}}{F_{st}} + x\right)^{n+1}} \tag{17}$$

The total spring rate is the summation of the spring rates of the piston side k_1 and rod side k_2, the total spring rate k_{total} can be written as:

$$ktotal = |k_1| + |k_2| = nF_{st} \left(\frac{\left(\frac{P_{up,pre}V_{up,pre}}{F_{st}}\right)^n}{\left(\frac{P_{up,pre}V_{up,pre}}{F_{st}} - x\right)^{n+1}} + \frac{\left(\frac{P_{dn,pre}V_{dn,pre}}{F_{st}}\right)^n}{\left(\frac{P_{dn,pre}V_{dn,pre}}{F_{st}} + x\right)^{n+1}} \right) \tag{18}$$

For the middle stroke position $x = 0$, the spring rate under static suspension load can be expressed as:

$$k_{total} = nF_{st}^2 \left(\frac{1}{P_{up,pre}V_{up,pre}} + \frac{1}{P_{dn,pre}V_{dn,pre}} \right) \tag{19}$$

The relationship between accumulator flow rate and hydraulic motor pressure difference can be expressed as:

$$Q_{acc} = C_d A_{acc} \sqrt{\frac{2 \mid \Delta P_m - P_{up,act}}{\rho}} \tag{20}$$

where Q_{acc} is the upstream accumulator flow rate, A_{acc} is the area of the accumulator inlet port, and ΔP_m is the pressure difference of the hydraulic motor.

2.2 Modelling of suspension cylinder and hydraulic rectifier

The governing equations of the HPEHS dynamic behaviour rely entirely on certain points, the charging and discharging processes of oil in the double-acting cylinder chambers, and the rotational motion of the hydraulic motor and generator. Figure 3 shows

a typical arrangement of the hydraulic rectifier circuit connection with the suspension cylinder and the flow directions through the hydraulic circuit during suspension system movement.

Figure 3 Schematic diagram of the hydraulic rectifier circuit and suspension cylinder (see online version for colours)

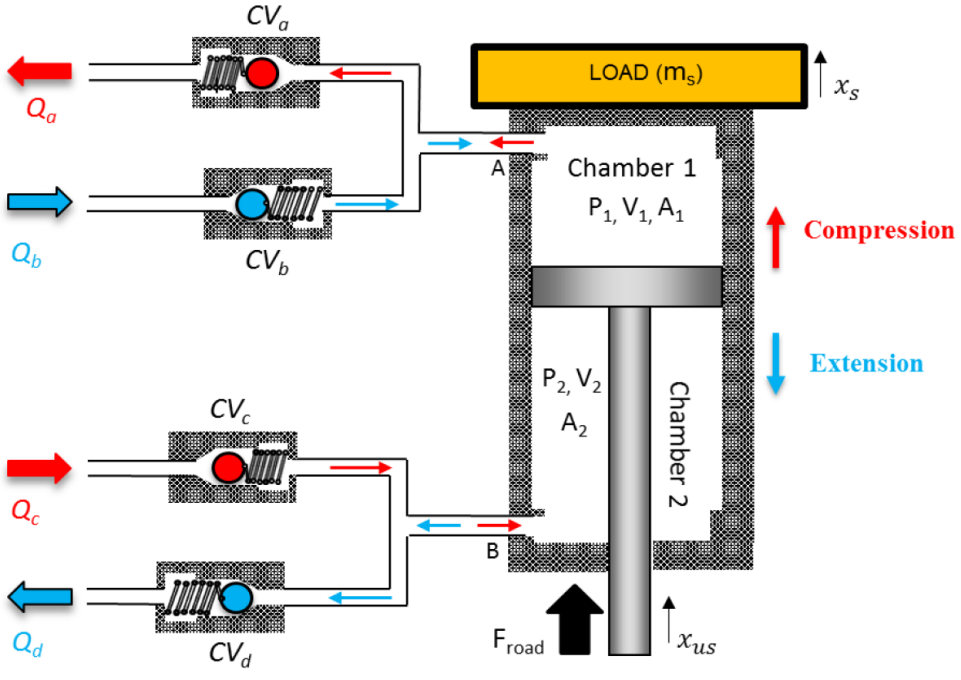

The input to the hydraulic cylinder is the excitation force F_{road} and the output is pressurised oil flow through both chambers. The forces on the cylinder as illustrated in Figure 3 can be expressed using Newton's second law of motion.

$$m_s\ddot{x}_s = ks\left(x_{us} - x_s\right) + \left(P_{2A2} - P_1A_1\right) + c\left(\dot{x}_{us} = \dot{x}_s\right) \tag{21}$$

where m_s is the sprung mass, k_s is the spring stiffness, x_{us} is the unsprung mass displacement, x_s is the sprung mass displacement, c is the viscous damping coefficient.

The hydraulic oil flow rate through the inlet port area of the check valves a, b, c and d can be described by the following equations:

$$Q_a = C_d A_{cv}\sqrt{\frac{2\left|P_1 - P_{up,ac} - P_{cv}\right|}{\rho}}, P_1 > P_{up,ac} + P_{cv} \tag{22}$$

$$Q_b = C_d A_{cv}\sqrt{\frac{2\left|P_{dn,ac} - P_2 - P_{cv}\right|}{\rho}}, P_{dn,ac} > P_2 + P_{cv} \tag{23}$$

$$Q_c = C_d A_{cv}\sqrt{\frac{2\left|P_2 - P_{up,ac} - P_{cv}\right|}{\rho}}, P_2 > P_{up,ac} + P_{cv} \tag{24}$$

$$Q_d = C_d A_{cv} \sqrt{\frac{2\left|P_{dn,ac} - P_1 = P_{cv}\right|}{\rho}}, P_{dn,ac} > P_1 + P_{cv} \tag{25}$$

where A_{cv} is the inlet port area of the check valve, C_d is the discharge coefficient, P_{cv} is the check valve opening pressure, ρ is the hydraulic fluid density, and $P_{up,ac}$ is the pressure inside accumulators 1 under the road vibration force.

2.3 Modelling of hydraulic motor

The dynamic relationship between the hydraulic motor flow rate Q_m and the pressure difference across the hydraulic motor ΔP_m can be described by the following equation:

$$Q_m = D_m \omega_m + K_L \Delta P_m \tag{26}$$

where, D_m is the hydraulic motor displacement, ω_{motor} is the angular velocity of the hydraulic motor shaft, K_L is the leakage coefficient.

The relationship between the hydraulic motor torque T_m and the pressure difference of the hydraulic motor can be expressed as:

$$T_m = D_m \Delta P_m \eta_{mech} \tag{27}$$

where η_{mech} is the mechanical efficiency of the hydraulic motor. The rotation speed ω_m of the hydraulic motor shaft can be calculated based on Newton's second law according to the following equation:

$$\omega_m = \frac{T_m - T_e - T_F - B_m \omega_m}{JT} \tag{28}$$

where T_e is the electromagnetic torque, B_m is the viscous friction coefficient of the hydraulic motor, T_F is the coulomb friction torque of the hydraulic motor, and J_T is the total moment of inertia on the shaft.

2.4 Modelling of the electromagnetic generator

The schematic diagram of the hydraulic motor, electromagnetic generator, and the external load resistance R_L is shown in Figure 1. The electromagnetic generator output voltage u_{emf} is given by:

$$u_{emf} = K_e \omega_m \tag{29}$$

where, K_e is the EMF constant of the electromagnetic generator. The relationship between the electromagnetic torque T_e and output current I of the electromagnetic generator can obtain the following equation:

$$T_e = K_t i \tag{30}$$

where, K_t is the torque constant of the electromagnetic generator. Based on Kirchhoff's voltage law, the electromagnetic generator output voltage U_{emf} cab be expressed as:

$$u_{emf} = i\left(R_{in} + R_L\right) + L_{in} \frac{di}{dt} \tag{31}$$

where R_{in} and L_{in} are the internal resistance and internal inductance of the electromagnetic generator.

2.5 The regenerated power conversion efficiency

The hydro-pneumatic energy harvesting suspension system provides the required damping force and harvests energy simultaneously from the road excitation force. The input power subjected to the hydraulic cylinder can be calculated as a function of piston forces and instantaneous velocity of the hydraulic cylinder according to the following equation.

$$P_{in} = F_1 \mid v(t) \mid_{co} + F_2 \mid v(t) \mid_{ex} \tag{32}$$

where, P_{in} is the input power to the hydraulic cylinder, F_1 is the piston force acting on chamber A during compression, F_2 is the piston force acting on chamber B during extension, and $v(t)$ is the instantaneous velocity of the hydraulic cylinder.

The energy harvesting power from the electromagnetic generator P_{out} can be calculated as a function of electric current and load resistance according to the following equation.

$$P_{out} = i^2 \left(R_{load} + R_{in} \right) \tag{33}$$

The total efficiency of the system can be expressed as follows:

$$\eta_{total} = \frac{P_{out}}{P_{in}} \tag{34}$$

The hydro-pneumatic energy harvesting suspension system has been modelled in detail using the block diagram-oriented environment, SIMULINK. The model of the HPEHS system is shown in Figure 4, there are five main blocks: hydraulic cylinder, hydraulic rectifier, accumulators, hydraulic motor, and generator. The suspension system parameters used in the simulation model and experimental setup are listed in Table 1.

Figure 4 Block diagram of the hydro-pneumatic energy harvesting suspension system

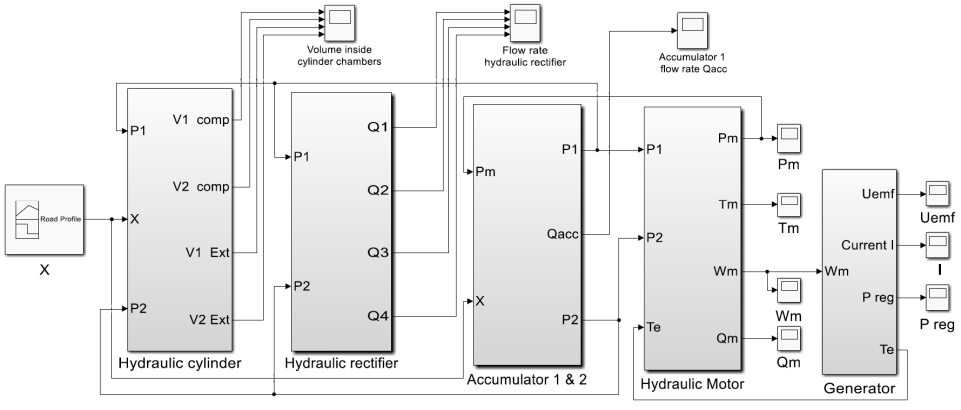

Table 1 Parameters of the HPEHS system

	Description	*Symbol*	*Value*	*Unit*
Hydraulic motor	Viscous friction coefficient	B_m	1.78 e-4	N m s/rad
	Displacement	D_m	8.2 e-6	m^3/rev
	Total moment of inertia	J_T	1.75 e-5	$kg.m^2$
	Coulomb friction torque	T_F	2.5 e-3	Nm
	Mechanical efficiency	η_{ech}	0.85	----
Hydraulic oil	Discharge coefficient	C_d	0.7	-----
	Kinematic viscosity	σ	22 e-6	m^2/s
	Density	ρ	872	kg/m^3
Shock absorber	Piston diameter	D_α	0.05	m
	Rod diameter	D_b	0.02	m
	Full stroke	x_{Full}	0.2	m
Check valve	Cracking pressure	P_{cv}	0.07	MPa
	Diameter	D_{cv}	0.01	m
Tyre	Stiffness	k_t	180,000	N/m
	Damping rate	c_t	1,000	N s/m
Electromagnetic generator	Electromagnetic voltage constant	K_e	0.25	V s/rad
	Electromagnetic torque constant	KT	0.25	N m/A
	Internal inductance	Lin	0.015	H
	External load resistor	R_{load}	10	Ω
	Internal resistance	R_{in}	5.32	Ω
Quarter-vehicle	Static suspension force	F_{st}	294	N
	Sprung mass	m_s	300	kg
	Unsprung mass	m_{us}	30	kg
Accumulators	Inlet port diameter	D_{acc}	0.012	m
	Specific heat ratio	n	1.4	----
	Upstream accumulator pre-charge pressure	$P_{up,pre}$	1	MPa
	Downstream accumulator pre-charge pressure	$P_{dn,pre}$	0.2	MPa
	Upstream accumulator volume	$V_{up,pre}$	0.5	L
	Downstream accumulator volume	$V_{dn,pre}$	0.75	L

3 Experimental test rig

A versatile quarter car test rig of the HPEHS is designed. The proposed design allows the installation and testing of a variety of different actual suspension devices. Figure 5 shows the main components of the proposed design of the test rig. It includes the frame, linear rails, bearings, moving mass, suspension cylinder, tyre, and actuator cylinder. The layout-based assembly design of the quarter car test rig is shown in Figure 6. The quarter

car test rig is designed and tested using SolidWorks to ensure that the device requirements have been met. The construction of the quarter car test rig is divided into three main hydraulic circuits. The first circuit is the hydraulic excitation circuit represents the road profile and excitation of the system. The second circuit is a regenerative hydro-pneumatic suspension circuit. And the third circuit is the variable hydraulic load circuit, which represents the weight of the vehicle.

3.1 Hydraulic excitation circuit

The hydraulic excitation circuit representing road vibrations consists of an electric motor, gear pump, oil tank, oil filter, pressure relief valve, and pressure gauge. The hydraulic power unit is connected to the double-acting cylinder through a 4/3 directional control valve to allow the reciprocatory motion for the excitation cylinder. The directional control valve input signal is controlled by the voltage signal from an analog output block of MATLAB. The input voltage value of the directional control valve changes from 0 to 5 volts to control the oil flow through the valve and the motion of the excitation cylinder.

3.2 Regenerative hydro-pneumatic suspension circuit

The main components of the regenerative hydro-pneumatic suspension circuit are the suspension cylinder, high-pressure accumulator, low-pressure accumulator, hydraulic rectifier, hydraulic motor, and an electric generator. The hydraulic rectifier consists of four check valves to rectify the bidirectional flow to the unidirectional flow during compression and extension stages. Two hydraulic accumulators with a capacity of 0.5 litres and 0.75 litres are connected to the high-pressure line and the low-pressure line, respectively. During the compression stage, the compressed oil flows from port A of the suspension cylinder to the high-pressure accumulator through check valve a. Then, the oil passes through the hydraulic motor and returns to the low-pressure accumulator to compensate for the oil shortage in the circuit. Next, the oil is returned to port B of the cylinder via check valve c. During the extension stage, the hydraulic cycle is reversed while maintaining the same direction of oil flow through the hydraulic motor. It should be noted that there is a damping force in the hydraulic circuit due to the presence of the check valves and the hydraulic motor. Also, the accumulator works as a pneumatic spring to generate the required stiffness force for the system and reduces pressure fluctuation in the system. Finally, the hydraulic motor shaft drives the electric generator to generate electric power.

Pressure transducers and pressure gauges are installed in the high-pressure line and low-pressure line to measure and monitor the inlet pressure and outlet pressure of the hydraulic motor. EVS 3100 HYDAC flow rate transmitter is installed before the hydraulic motor inlet port to measure the actual flow rate to calculate the hydraulic power. A rotary encoder is attached to the hydraulic motor shaft to measure the output rotation speed.

ACS712 current sensor is used to measure the output current of the harvested power. The road excitation circuit is the source of suspension system vibration through the tyre pan where the wheel disk of the quarter car is attached to the piston rod of the suspension cylinder. LWH-225 position transducer is fixed on the sprung mass plate to measure the displacement of the sprung mass.

All signals from transducers are sent to the computer via a National Instruments USB-6221 DAQ card through an A/D converter terminal. The DAQ card has 16 analogue inputs and two analogue outputs with a sampling rate of 250 kS/s, and an input voltage range of ±10 V.

3.3 Hydraulic load circuit

The total weight of the sprung mass consists of the variable hydraulic load and the weight of the moving plate which is approximately 100 kg. The variable hydraulic load circuit consists of a double-acting cylinder, throttle check valve, pressure gauge, and oil tank as shown in Figure 7. The load cylinder is fixed to the frame and the sprung mass plate by two joints. The lower inlet port of the cylinder is connected to the oil tank through a throttle check valve to control the oil flow. The design of the hydraulic loading system allows for testing different types and sizes of suspension systems with different loads.

Figure 5 Test rig setup (see online version for colours)

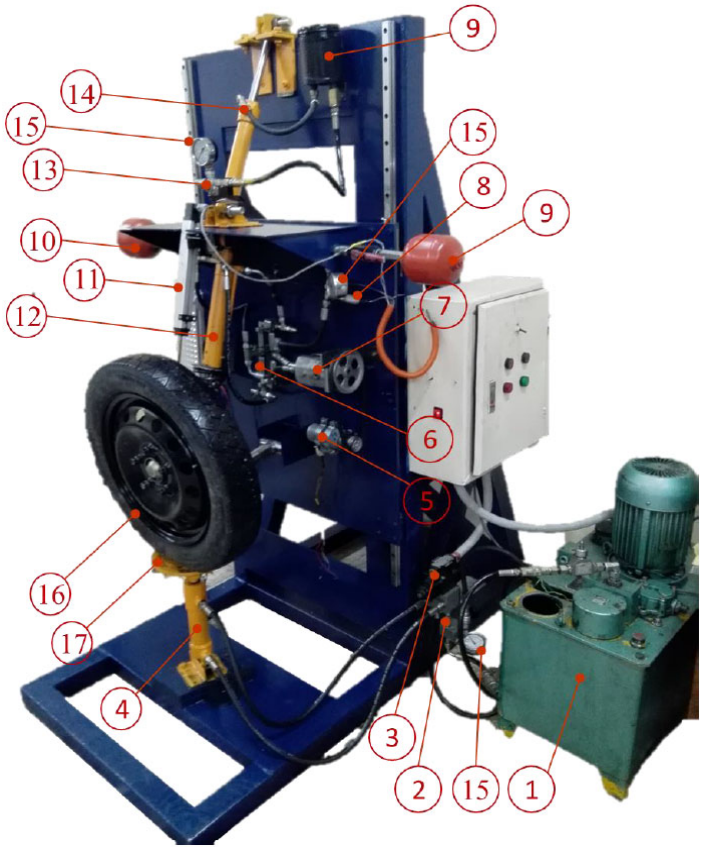

Notes: Hydraulic power unit (1) pressure relief valve (2) directional control valve (3) excitation cylinder (4) generator (5) hydraulic rectifier (6) hydraulic motor (7) pressure transducers (8) high-pressure accumulator (9) low-pressure accumulator (10) position transducer (11) suspension cylinder (12) throttle valve (13) load cylinder (14) gauge (15) wheel (16) Pan (17)

Figure 6 Isometric view of the HPEHS system (see online version for colours)

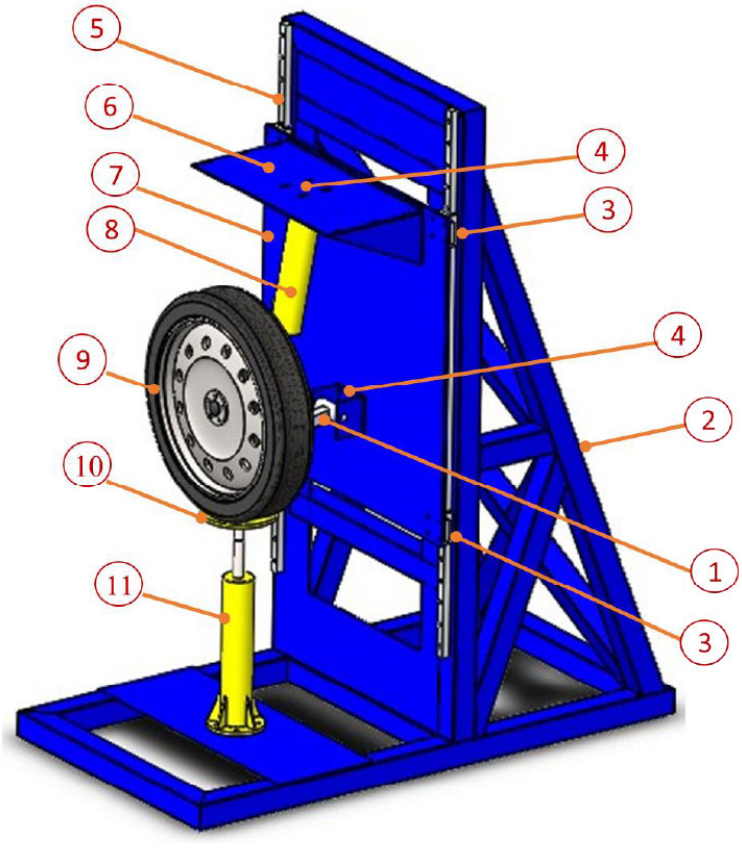

Notes: Suspension arm (1) frame (2) rolling bearings (3) suspension fixation (4) linear rails (5) sprung mass plate (6) movable plate (7) suspension cylinder (8) tyre and wheel (9) tyre pan (10) actuator cylinder (11)

Figure 7 The schematic diagram of the hydraulic load circuit (see online version for colours)

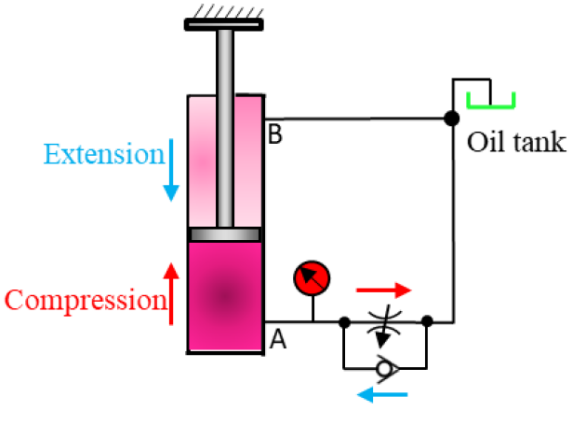

4 Experimental and simulation results (experimental validation)

Figure 8 to Figure 11 show the comparison between the simulation and experimental responses of the high-pressure line, hydraulic motor shaft speed, hydraulic flow rate, and hydraulic output power of the HPEHS system, respectively. The validation results show that the model has a good representation of the real system.

Figure 8 The simulation and experimental responses of the high-pressure line (see online version for colours)

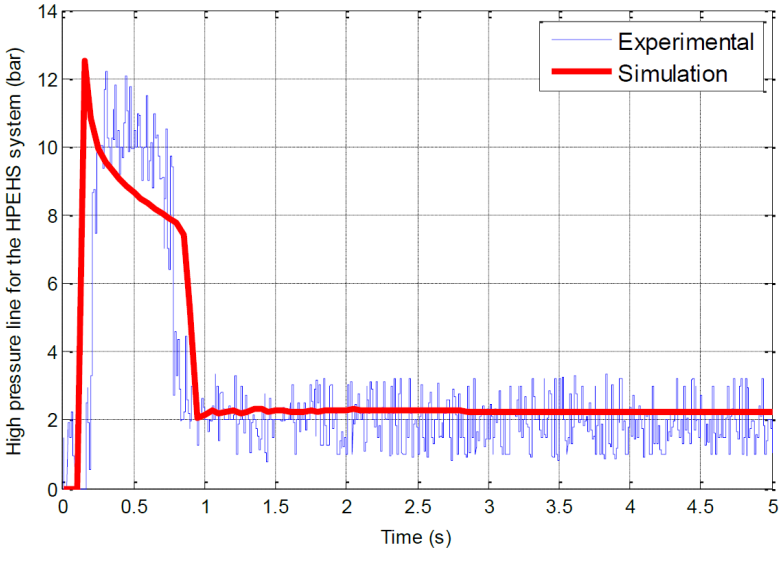

Figure 9 The simulation and experimental responses of the hydraulic motor shaft speed (see online version for colours)

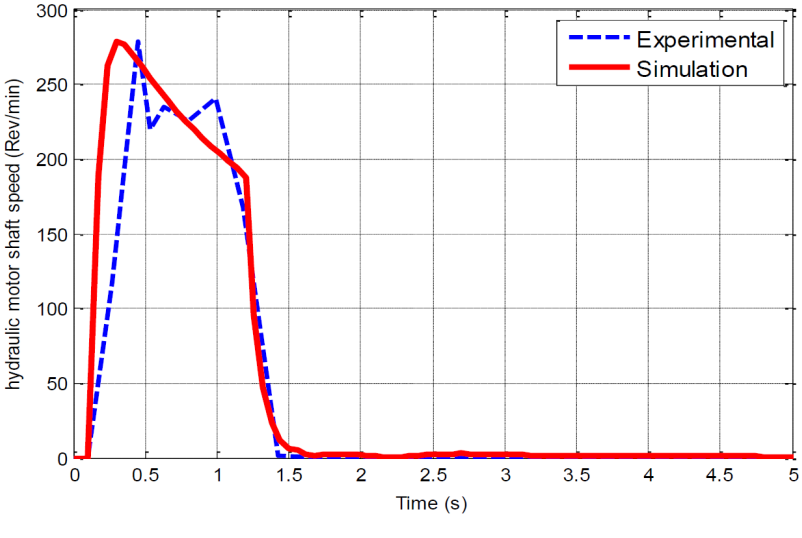

Figure 10 The simulation and experimental responses of the hydraulic flow rate (see online version for colours)

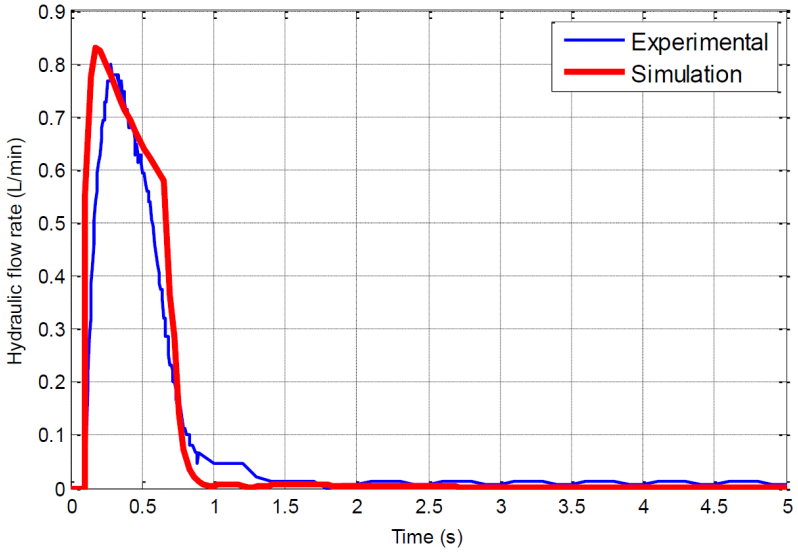

Figure 11 The simulation and experimental responses of the hydraulic output power of the HPEHS system (see online version for colours)

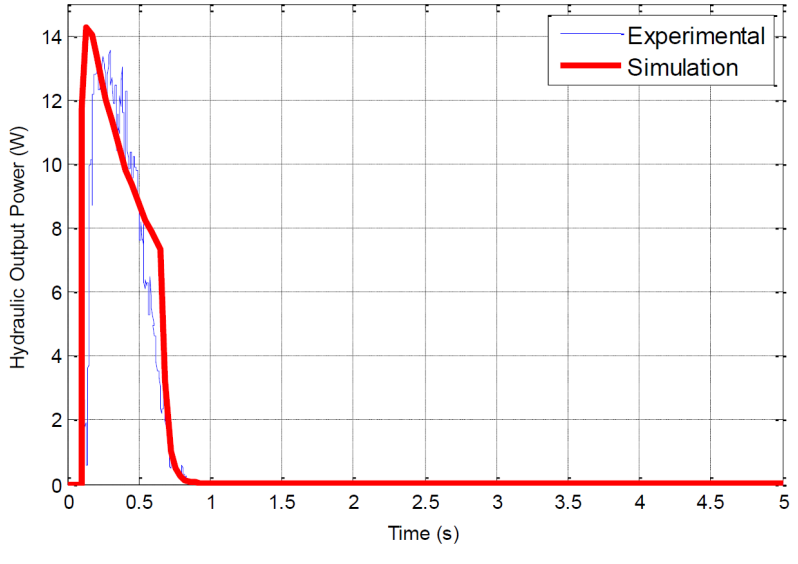

4.1 Effect of the sprung mass

The effect of the sprung mass (load) on the performance of the HPEHS system and the harvested power is tested using different loads of 250 kg, 300 kg, and 350 kg. The load value is changed by adjusting the hydraulic load circuit pressure by the throttle control valve. Figure 12 to Figure 15 show the variation of the sprung mass displacement, high-

pressure line, hydraulic motor shaft speed, and harvested power of the HPEHS system for different loads. The results show that as the sprung mass load increases the harvested power and the motor speed increases, on the contrary, it reduces the displacement of the sprung mass.

Figure 12 Variation of sprung mass displacement of the HPEHS system with different loads (see online version for colours)

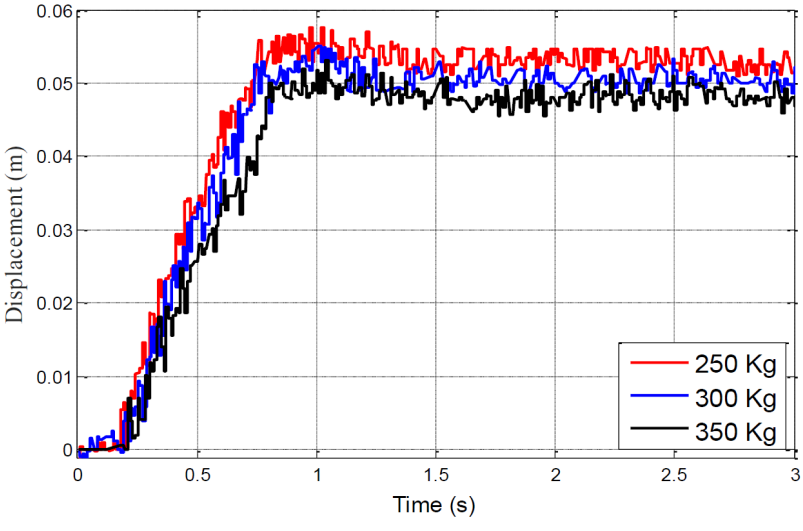

Figure 13 Variation of the high-pressure line of the HPEHS system with different loads (see online version for colours)

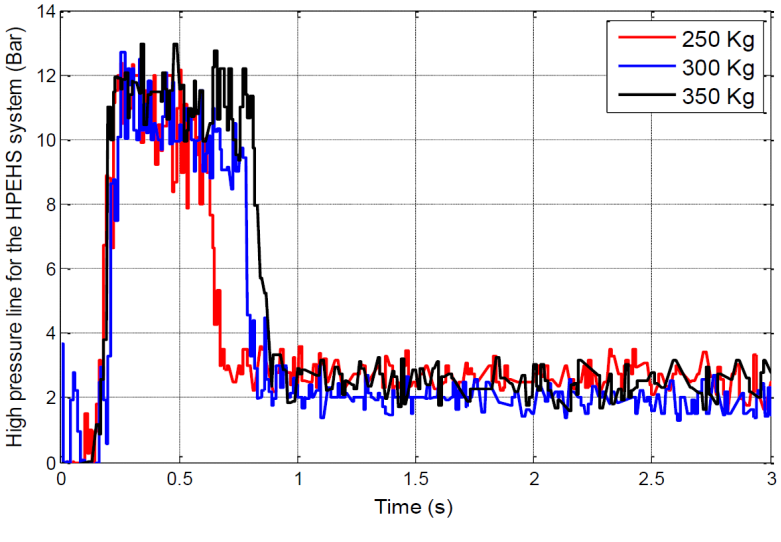

Figure 14 Variation of the hydraulic motor shaft speed of the HPEHS system with different loads (see online version for colours)

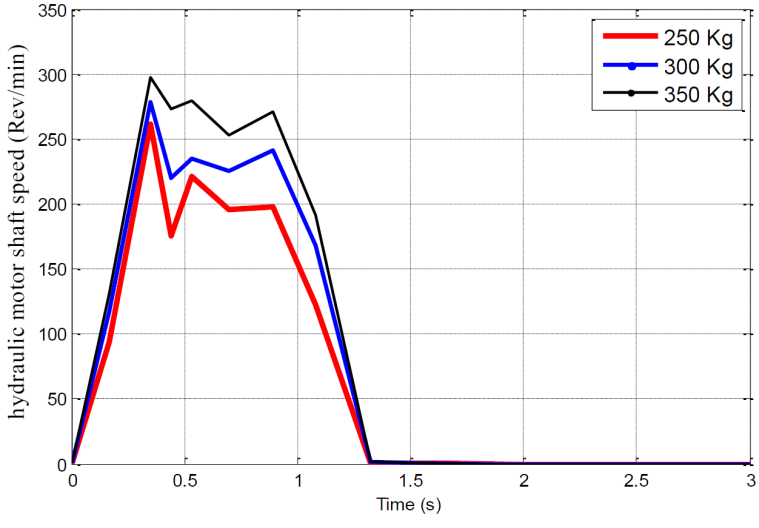

Figure 15 Variation of the harvested power of the HPEHS system with different loads (see online version for colours)

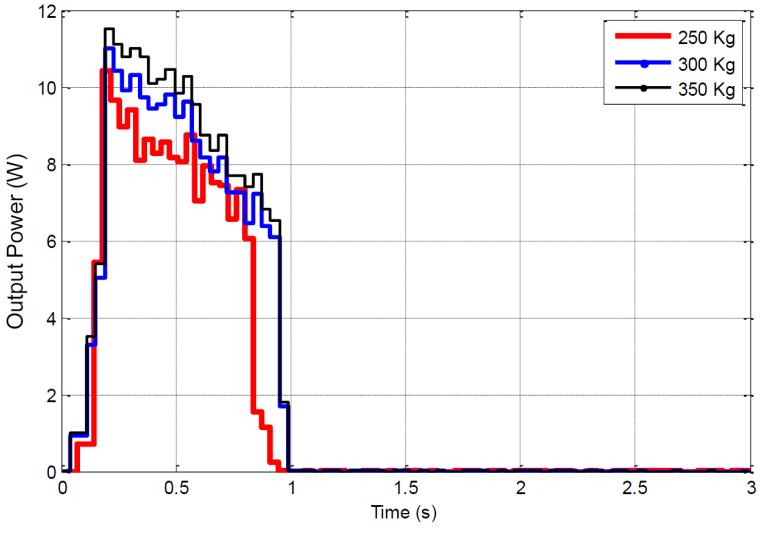

4.2 Effect of the accumulator

To investigate the significance of the accumulators on the performance of the HPEHS system and harvested power, the system is tested with and without accumulators. Figure 16 to Figure 19 show the variation of the system displacement, high-pressure line, hydraulic motor shaft speed, and harvested power of the HPEHS system with and without accumulators, respectively. It is clear that the system with the accumulators increases the

stability of the sprung mass and minimises the pressure fluctuation to ensure the stability of the hydraulic motor rotation to achieve the maximum harvested power.

Figure 16 Displacement variation of the HPEHS system with and without accumulators (see online version for colours)

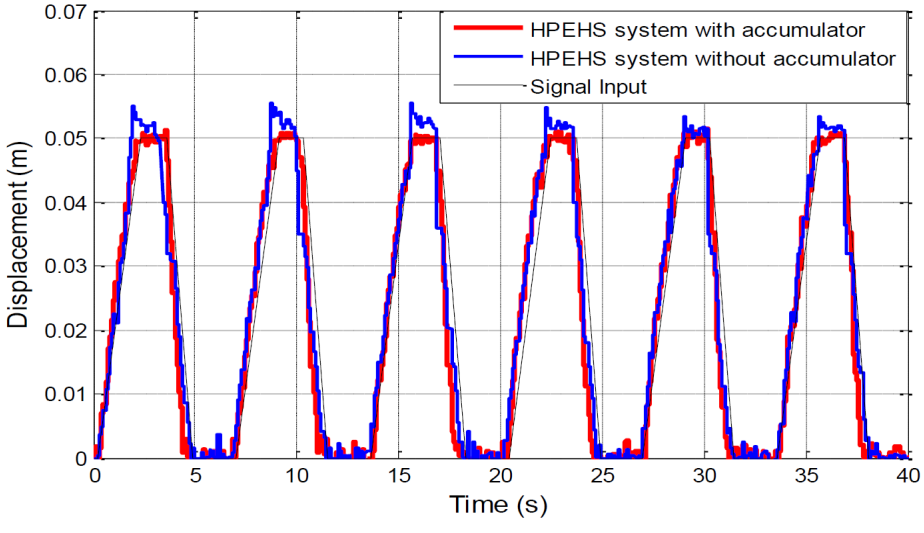

Figure 17 Variation of the high-pressure line of the HPEHS system with and without accumulators (see online version for colours)

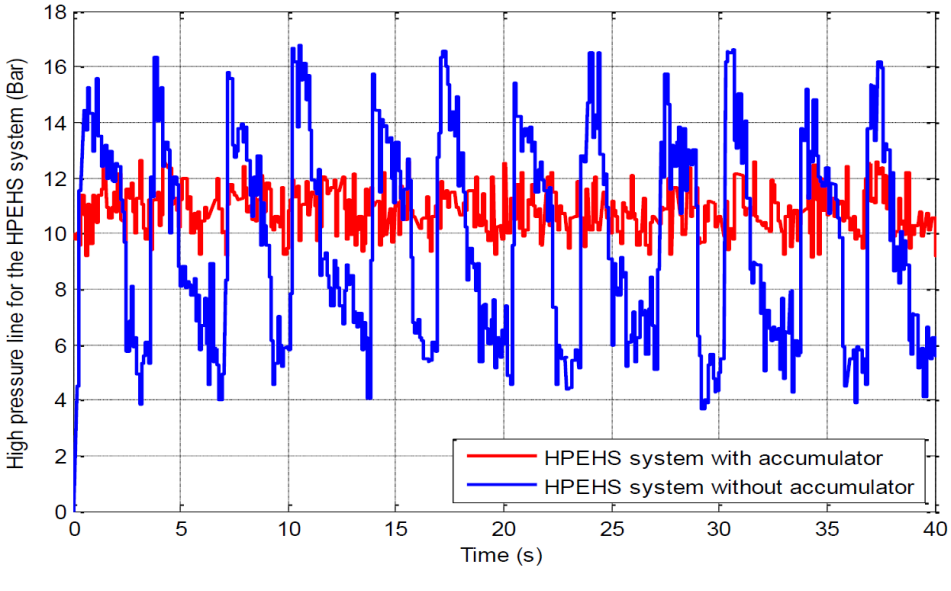

Figure 18 Variation of the hydraulic motor shaft speed of the HPEHS system with and without accumulators (see online version for colours)

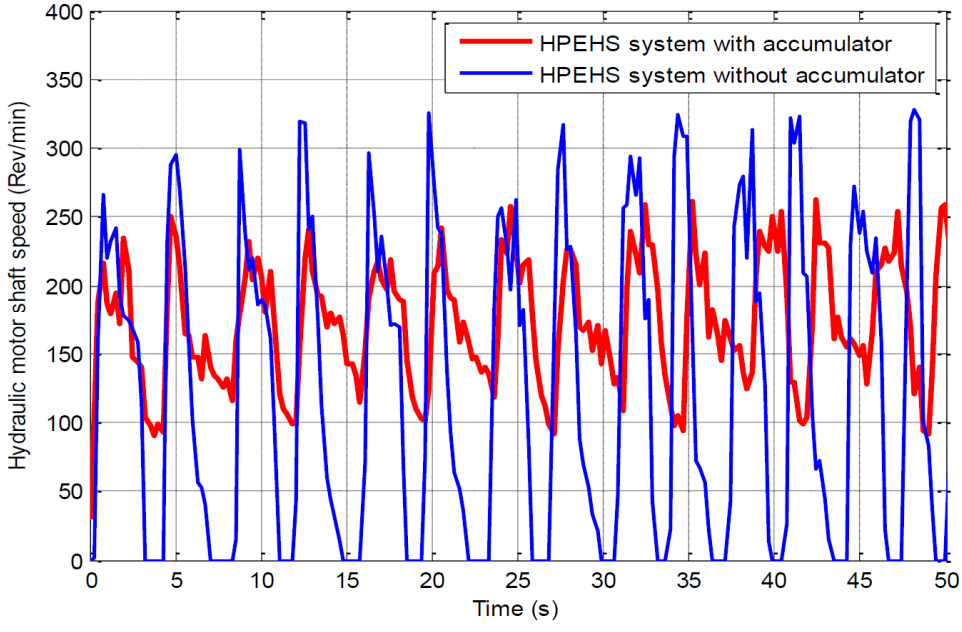

Figure 19 Variation of the harvested power of the HPEHS system with and without accumulators (see online version for colours)

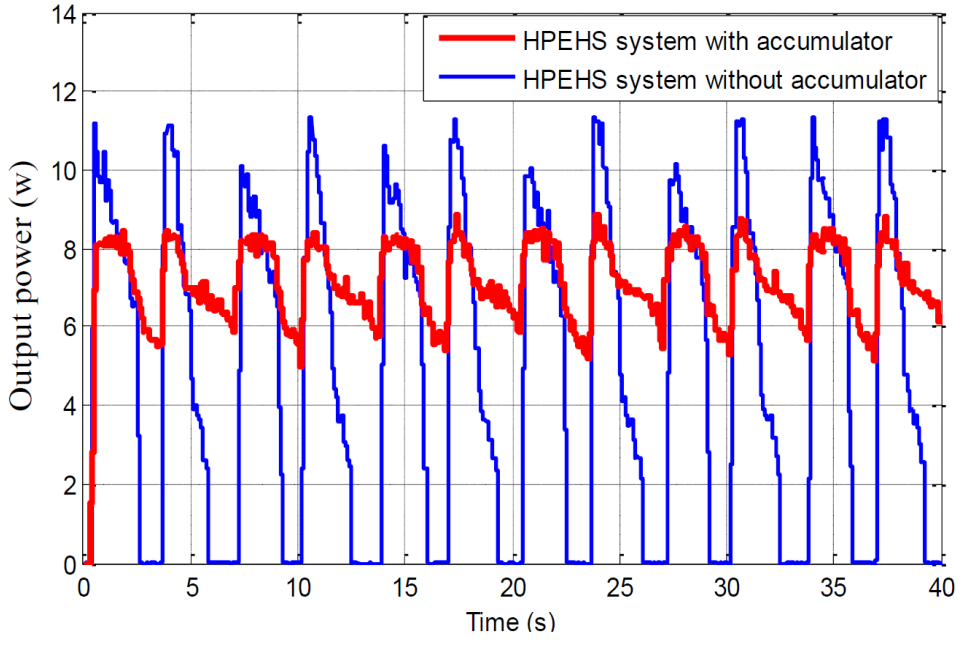

5 Conclusions

A promising experimental setup of a quarter car HPEHS has been carried out to discuss the performance of the system and the amount of harvested power that can be gained from the vehicle suspension vibration. A mathematical model based on MATLAB-Simulink for the regenerative suspension system was performed to validate the experimental results. The variables discussed in the study were the high-pressure line, hydraulic motor shaft speed, hydraulic flow rate, and hydraulic output power of the HPEHS system. From the research that has been carried out and the results obtained, it is possible to conclude that the simulation results thus obtained agree with the real measurements. The sprung mass and the hydro- pneumatic accumulator have a great effect on the system. The effect of the sprung mass (load) on the performance of the HPEHS system and the harvested power is tested using different loads of 250 kg, 300 kg, and 350 kg. Also to identify the importance of the accumulator on the performance of the HPEHS system and harvested power, the system is tested with and without accumulators. In conclusion, it is evident that as the sprung mass load increases the motor speed and the harvested power on the contrary, it reduces the displacement of the sprung mass. The accumulator minimises the fluctuation in system pressure and motor speed and increases the stability of the suspension system which leads to achieving maximum harvested power. The average power of the regenerative suspension system is approximately 7.5 W.

References

Awad, M.N. and Me El-Arabi, S.A.R. (2021) 'Identification and analysis of servo-pneumatic system using mixed reality environment', *Journal of International Society for Science and Engineering*, Vol. 3, No. 3, pp.43–48.

Awad, M.N., Sokar, M.I., Abdrabbo, S.M. and El-Arabi, M.E-S. (2018a) 'Hydro-pneumatic energy harvesting suspension system using a PSO based PID controller', *SAE International Journal of Commercial Vehicles*, Vol. 11, No. 4, pp.223–234.

Awad, M.N., Sokar, M.I., Rabbo, S.A. and El-Arabi, M. (2018b) 'Performance evaluation and damping characteristics of hydro-pneumatic regenerative suspension system', *International Journal of Applied Engineering Research*, Vol. 13, No. 7, pp.5436–5442.

Berg, N.I., Holm, R.K. and Rasmussen, P.O. (2014) 'A novel magnetic lead screw active suspension system for vehicles', *2014 IEEE Energy Conversion Congress and Exposition (ECCE)*, IEEE, pp.3139–3146.

Cassidy, I.L., Scruggs, J.T., Behrens, S. and Gavin, H.P. (2011) 'Design and experimental characterization of an electromagnetic transducer for large-scale vibratory energy harvesting applications', *Journal of Intelligent Material Systems and Structures*, Vol. 22, No. 17, pp.2009–2024.

Chen, C., Chan, Y.S., Zou, L. and Liao, W-H. (2018) 'Self-powered magnetorheological dampers for motorcycle suspensions', *Proceedings of the Institution of Mechanical Engineers, Part D: Journal of Automobile Engineering*, Vol. 232, No. 7, pp.921–935.

Galluzzi, R., Xu, Y., Amati, N. and Tonoli, A. (2018) 'Optimized design and characterization of motor-pump unit for energy-regenerative shock absorbers', *Applied Energy*, Vol. 210, pp.16–27.

Guo, S., Liu, Y., Xu, L., Guo, X. and Zuo, L. (2016) 'Performance evaluation and parameter sensitivity of energy-harvesting shock absorbers on different vehicles', *Vehicle System Dynamics*, Vol. 54, No. 7, pp.918–942.

Gysen, B.L.J., Van Der Sande, T.P.J., Paulides, J.J.H. and Lomonova, E.A. (2011) 'Efficiency of a regenerative direct-drive electromagnetic active suspension', *IEEE Transactions on Vehicular Technology*, Vol. 60, No. 4, pp.1384–1393.

Hao, L. and Namuduri, C. (2013) 'Electromechanical regenerative actuator with fault-tolerance capability for automotive chassis applications', *IEEE Transactions on Industry Applications*, Vol. 49, No. 1, pp.84–91.

Huang, B., Hsieh, C-Y., Golnaraghi, F. and Moallem, M. (2015) 'Development and optimization of an energy-regenerative suspension system under stochastic road excitation', *Journal of Sound and Vibration*, Vol. 357, pp.16–34.

Kim, B-S., Lee, D-W. and Kwon, S-J. (2016) 'Vehicle dynamic analysis for the ball-screw type energy harvesting damper system', *International Conference on Advanced Engineering Theory and Applications*, Springer, pp.853–862.

Li, C., Zhu, R., Liang, M. and Yang, S. (2014) 'Integration of shock absorption and energy harvesting using a hydraulic rectifier', *Journal of Sound and Vibration*, Vol. 333, No. 17, pp.3904–3916.

Li, P. and Zuo, L. (2013) 'Assessment of vehicle performances with energy-harvesting shock absorbers', *SAE International Journal of Passenger Cars-Mechanical Systems*, Vol. 6, No. 1, pp.18–27.

Li, Z., Zuo, L., Kuang, J. and Luhrs, G. (2013a) 'Energy-harvesting shock absorber with a mechanical motion rectifier', *Smart Materials and Structures*, Vol. 22, No. 2, p.25008.

Li, Z., Zuo, L., Luhrs, G., Lin, L. and Qin, Y-X. (2013b) 'Electromagnetic Energy-Harvesting shock absorbers: design, modeling, and road tests', *IEEE Transactions on Vehicular Technology*, Vol. 62, No. 3, pp.1065–1074.

Liu, S., Wei, H. and Wang, W. (2011) *Investigation on Some Key Issues of Regenerative Damper With Rotary Motor for Automobile Suspension*, Vol. 3, pp.1435–1439.

Liu, Y., Xu, L. and Zuo, L. (2017) 'Design, modeling, lab, and field tests of a mechanical-motion-rectifier-based energy harvester using a ball-screw mechanism', *IEEE/ASME Transactions on Mechatronics*, Vol. 22, No. 5, pp.1933–1943.

Maravandi, A. and Moallem, M. (2015) 'Regenerative shock absorber using a two-leg motion conversion mechanism', *IEEE/ASME Transactions on Mechatronics*, Vol. 20, No. 6, pp.2853–2861.

Sabzehgar, R., Maravandi, A. and Moallem, M. (2014) 'Energy regenerative suspension using an algebraic screw linkage mechanism', *IEEE/ASME Transactions on Mechatronics*, Vol. 19, No. 4, pp.1251–1259.

Soares Dos Santos, M.P., Ferreira, J.A., Simoes, J.A., Pascoal, R., Torrao, J., Xue, X. and Furlani, E.P. (2016) 'Magnetic levitation-based electromagnetic energy harvesting: a semi-analytical non-linear model for energy transduction', *Sci. Rep.*, Vol. 6, p.18579.

Tonoli, A., Amati, N., Detoni, J. G., Galluzzi, R. and Gasparin, E. (2013) 'Modelling and validation of electromechanical shock absorbers', *Vehicle System Dynamics*, Vol. 51, No. 8, pp.1186–1199.

Xu, L., Liu, Y., Guo, S., Guo, X. and Zuo, L. (2015) 'Damping characteristics of a hydraulic electric rectifier shock absorber and its effect on vehicle dynamics', *17th International Conference on Advanced Vehicle Technologies; 12th International Conference on Design Education; 8th Frontiers in Biomedical Devices*, Vol. 3.

Zhang, G., Cao, J. and Yu, F. (2012) 'Design of active and energy-regenerative controllers for DC-motor-based suspension', *Mechatronics*, Vol. 22, No. 8, pp.1124–1134.

Zhang, R., Wang, X. and Liu, Z. (2018) 'A novel regenerative shock absorber with a speed doubling mechanism and its Monte Carlo simulation', *Journal of Sound and Vibration*, Vol. 417, pp.260–276.

Zhang, Y., Zhang, X., Zhan, M., Guo, K., Zhao, F. and Liu, Z. (2015) 'Study on a novel hydraulic pumping regenerative suspension for vehicles', *Journal of the Franklin Institute*, Vol. 352, No. 2, pp.485–499.

Zhang, Z., Zhang, X., Chen, W., Rasim, Y., Salman, W., Pan, H., Yuan, Y. and Wang, C. (2016) 'A high-efficiency energy regenerative shock absorber using supercapacitors for renewable energy applications in range extended electric vehicle', *Applied Energy*, Vol. 178, No. 1, pp.177–188.

Zhou, Q., Guo, X., Xu, L., Wang, G. and Zhang, J. (2015) *Simulation based Evaluation of the Electro-Hydraulic energy-Harvesting Suspension (EHEHS) for Off-Highway Vehicles*, Vol. 1, SAE Technical Paper, SAE, No. 2015-01-1494.

Zhu, S., Shen, W-A. and Xu, Y-L. (2012) 'Linear electromagnetic devices for vibration damping and energy harvesting: Modeling and testing', *Engineering Structures*, Vol. 34, pp.198–212.

Zuo, L. and Zhang, P-S. (2013) 'Energy harvesting, ride comfort, and road handling of regenerative vehicle suspensions', *Journal of Vibration and Acoustics*, Vol. 135, No. 4, pp.295–302.

Zuo, L., Scully, B., Shestani, J. and Zhou, Y. (2010) 'Design and characterization of an electromagnetic energy harvester for vehicle suspensions', *Smart Materials and Structures*, Vol. 19, No. 1, p.45003.